Auxiliary Random Finite Element Method for Risk Assessment of 3-D Slope

Te Xiao,[1] Dian-Qing Li, Ph.D., M.ASCE,[2] Zi-Jun Cao, Ph.D.,[3] Siu-Kui Au, Ph.D., M.ASCE,[4] and Xiao-Song Tang, Ph.D.[5]

[1]State Key Laboratory of Water Resources and Hydropower Engineering Science, Wuhan University, Wuhan 430072, P. R. China; e-mail: short_xiaote@whu.edu.cn
[2]State Key Laboratory of Water Resources and Hydropower Engineering Science, Wuhan University, Wuhan 430072, P. R. China; e-mail: dianqing@whu.edu.cn
[3]State Key Laboratory of Water Resources and Hydropower Engineering Science, Wuhan University, Wuhan 430072, P. R. China; e-mail: zijuncao@whu.edu.cn (corresponding author)
[4]Institute for Risk and Uncertainty, University of Liverpool, Liverpool L69 3GH, United Kingdom; e-mail: siu-kui.Au@liverpool.ac.uk
[5]State Key Laboratory of Water Resources and Hydropower Engineering Science, Wuhan University, Wuhan 430072, P. R. China; e-mail: xstang@whu.edu.cn

ABSTRACT

Spatial variability of soil properties is one of the major uncertainties in geotechnical properties that significantly affect slope reliability and risk. To account for the effect of three-dimensional (3-D) spatial variability, an efficient random finite element method (RFEM), named auxiliary RFEM (ARFEM), is proposed for 3-D slope reliability analysis and risk assessment. The ARFEM consists of two steps: the preliminary analysis using a relatively coarse 3-D finite-element model and subset simulation, and the target analysis using a detailed 3-D finite-element model and response conditioning method. Compared with direct Monte Carlo simulation-based RFEM, ARFEM can provide consistent reliability and risk estimates with much less computational efforts. In addition, it is found that both the horizontal and vertical spatial variability have significant, but different, impacts on 3-D slope reliability, risk and failure mechanisms.

INTRODUCTION

Spatial variability of soil properties is one of the major uncertainties in geotechnical properties that significantly affect slope reliability and risk. A majority of previous studies based on 2-D analysis (e.g., Griffiths and Fenton, 2004; Wang et al., 2011; Huang et al., 2013; Jha and Ching, 2013; Li et al., 2016a,b; Xiao et al., 2017) cannot account for the effect of spatial variability in the axial direction of slopes. Based on the 2-D analysis, slope fails along columnar slip surface with infinite length in 3-D space, which is inconsistent with the actual failure surface (i.e., irregular and finite) observed in slope engineering. Since the identification of slip surface is an

essential step for estimation of failure probability and failure consequence in slope risk assessment, it is necessary to combine 3-D slope stability analysis and 3-D spatial variability modeling to achieve more rigorous probabilistic analysis of 3-D slope stability.

In the past few decades, several approaches for 3-D slope reliability analysis were developed (e.g., Vanmarcke, 1977; Griffiths et al., 2009; Hicks et al., 2014; Ji and Chan, 2014). Among these approaches, random finite element method (RFEM) is considered as the most rigorous method, which combines Monte Carlo simulation (MCS) for uncertainty propagation, finite element (FE) method for slope stability analysis, and random field theory for spatial variability modeling. However, direct MCS-based RFEM often suffers from a criticism of requiring extensive computational efforts, particularly for 3-D slope risk assessment at small probability levels. Using a relatively coarse FE model (e.g., model with coarse FE mesh) in RFEM may be a feasible strategy to improve the computational efficiency, but it might not produce consistent results compared with a detailed FE model (e.g., model with fine FE mesh). It is interesting to explore the possibility that takes the advantages of both coarse FE model (i.e., computationally efficient) and fine FE model (i.e., theoretically accurate) in slope risk assessment so as to efficiently obtain consistent reliability and risk estimates.

This paper proposes an efficient RFEM, named auxiliary RFEM (ARFEM), for 3-D slope reliability analysis and risk assessment, in which both coarse and fine FE models are adopted in different stages of analysis. With the aid of ARFEM, this paper focuses on exploring the effects of spatial variability, including both horizontal and vertical ones, on reliability, risk and failure mechanisms of 3-D slope.

AUXILIARY RANDOM FINITE ELEMENT METHOD

The coarse and fine FE models are adopted in ARFEM for different purposes, which constitute two steps of ARFEM, namely preliminary analysis and target analysis, as illustrated in Figure 1. The preliminary analysis adopts a relatively coarse FE model and subset simulation (SS) (Au and Wang, 2014) to efficiently, but approximately, assess slope reliability and risk. Based on the information (i.e., the sample space partition) generated in the preliminary analysis, the target analysis utilizes a fine FE model and response conditioning method (RCM) (Au, 2005) to achieve efficient and consistent reliability and risk assessment.

Step 1: Preliminary Analysis. For slope stability problem, engineers are concerned with the probability, P_f, and risk, R, that the safety factor of slope stability, FS, is smaller than a given threshold fs (e.g., $fs = 1$). This is usually a rare event for a well-designed slope. By performing an SS run with m simulation levels, the sample space is divided into $m+1$ mutually exclusive and collectively exhaustive subsets Ω_k, $k = 0, 1, \ldots, m$, according to the safety factors calculated using the coarse FE model, FS_p. Let p_0 be the conditional probability in SS and N be the sample size in each simulation level. The occurrence probability of Ω_k, $P(\Omega_k)$, is taken as $p_0^k(1-p_0)$ for $k = 0, 1, \ldots, m-1$, and p_0^k for $k = m$, and the number of random samples falling into Ω_k, N_k, equals

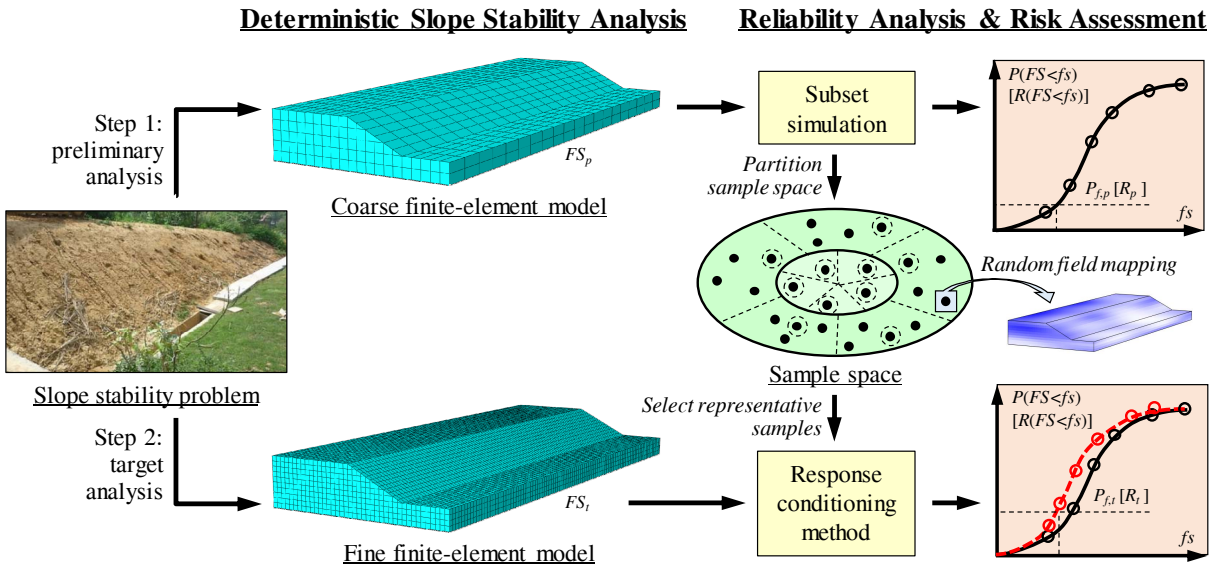

Figure 1. Schematic diagram of auxiliary random finite element method.

to $N(1-p_0)$ for $k = 0, 1, \ldots, m-1$, and Np_0 for $k = m$. Using these SS samples, the preliminary slope failure probability, $P_{f,p}$, and preliminary slope failure risk, R_p, based on the coarse FE model can be calculated as (Xiao et al., 2016)

$$P_{f,p} = \sum_{k=0}^{m}\sum_{j=1}^{N_k} I_{p,kj}\frac{P(\Omega_k)}{N_k} \tag{1}$$

$$R_p = \sum_{k=0}^{m}\sum_{j=1}^{N_k} C_{p,kj}\frac{P(\Omega_k)}{N_k} \tag{2}$$

where $I_{p,kj}$ and $C_{p,kj}$ are failure indicator function and failure consequence corresponding to j-th sample in Ω_k based on coarse FE model, respectively. If corresponding $FS_{p,kj} < fs$, $I_{p,kj} = 1$ and $C_{p,kj}$ needs to be estimated additionally; otherwise, $I_{p,kj} = C_{p,kj} = 0$. It can be proved that Equation (2) equals to the conventional definition of R, namely $R = P_f \times \bar{C}$ (Li et al., 2016a), where $\bar{C}$ is the average slope failure consequence.

Although preliminary analysis with coarse FE model only provides approximate estimates of P_f and R, it can be finished with acceptable computational effort in practice and provides valuable information and insights (e.g., Ω_k, $k = 0, 1, \ldots, m$, and random samples in these subsets) for understanding the slope stability problem. Such information is incorporated into more realistic fine FE model-based target analysis to obtain the refined and consistent reliability and risk estimates, as provided in the next section.

Step 2: Target Analysis. Since samples in their close neighborhood may have similar performances, it is reasonable to select a part of samples as the representative samples in small sample space as shown in Figure 1, which is referred as the sub-binning strategy in RCM (Au, 2007). Concretely, Ω_k is further divided into N_s ($N_s << N$) equal sub-bins Ω_{kj}, $j = 1, 2, \ldots, N_s$, according to the FS_p values. One of N_k/N_s samples in each Ω_{kj} is then randomly selected as a

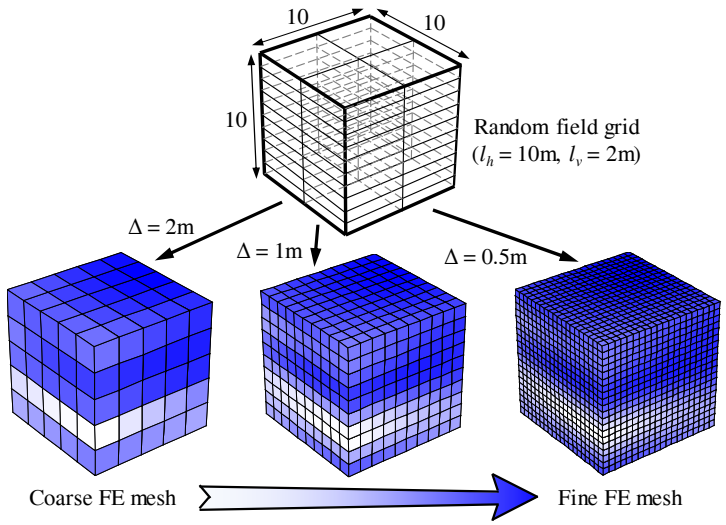

Figure 2. Identical random field realization mapped onto different FE meshes.

representative sample and is used as input of the fine FE model to recalculate the safety margin of slope stability. By this means, the target slope failure probability, $P_{f,t}$, and target slope failure risk, R_t, based on the fine FE model are calculated as (Xiao et al., 2016)

$$P_{f,t} = \sum_{k=0}^{m} \sum_{j=1}^{N_s} I_{t,kj} \frac{P(\Omega_k)}{N_s} \tag{3}$$

$$R_t = \sum_{k=0}^{m} \sum_{j=1}^{N_s} C_{t,kj} \frac{P(\Omega_k)}{N_s} \tag{4}$$

where $I_{t,kj}$ and $C_{t,kj}$ are failure indicator function and failure consequence corresponding to the representative sample in Ω_{kj} based on fine FE model, respectively. Similarly, if corresponding $FS_{t,kj} < fs$, $I_{t,kj} = 1$ and $C_{t,kj}$ needs to be estimated additionally; otherwise, $I_{t,kj} = C_{t,kj} = 0$.

From preliminary analysis to target analysis, only $mN(1-p_0)+Np_0$ coarse FE analyses and $(m+1)N_s$ fine FE analyses are required in ARFEM. Compared with directly performing MCS or SS based on fine FE model, the total computational effort of ARFEM is substantially reduced. More importantly, those estimates can be proved to be asymptotically unbiased (Au, 2007). The advantages of both coarse FE model (i.e., computationally more efficient) and fine FE model (i.e., theoretically more accurate) are properly integrated through ARFEM.

Spatial Variability Modeling. Two steps of ARFEM necessitate the same sample space so that random samples generated in preliminary analysis can be directly used in target analysis (see Figure 1). This is not trivial when spatial variability of soil properties is considered because FE meshes in coarse and fine FE models are different. To address this problem, the expansion optimal linear estimation approach (Sudret and Der Kiureghian, 2000) is adopted in ARFEM to generate random field for 3-D spatial variability modeling. Random field is first generated on a set of grid determined by the accuracy of random field mapping, and is then mapped onto different FE meshes determined by the accuracy of FE analysis, as shown in Figure 2. Note that

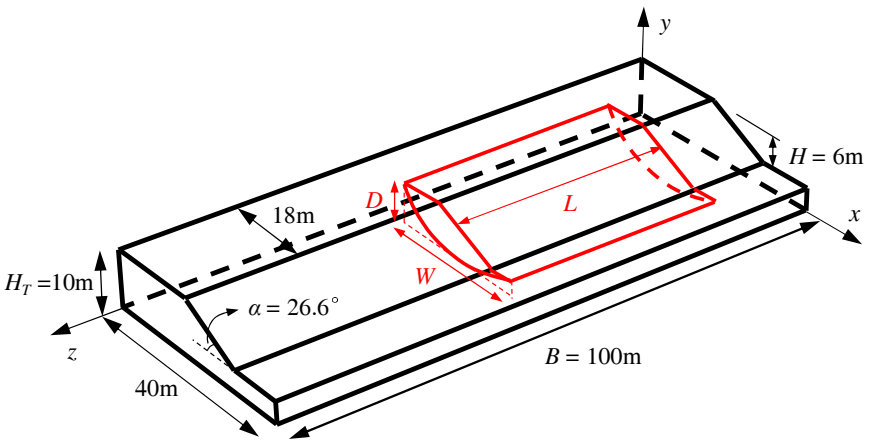

Figure 3. Illustrative slope example.

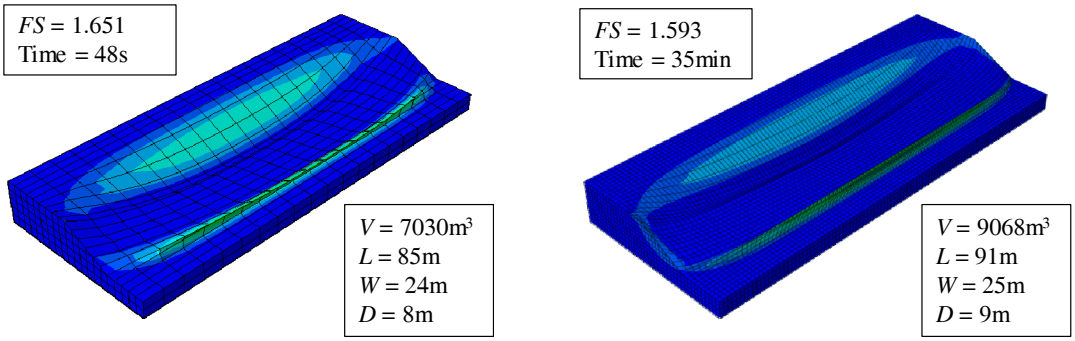

(a) Coarse FE model (b) Fine FE model

Figure 4. Deterministic slope stability analysis results.

no variance reduction is considered in this study, because the random field is generated and mapped at the point level. By this means, the sample space is related to the random field grid that remains unchanged in coarse and fine FE models, rather than related to the FE mesh. This makes it possible to share random samples in the two steps of ARFEM.

ILLUSTRATIVE 3-D SLOPE EXAMPLE

For illustration, this section applies ARFEM to evaluating the failure probability and risk of a 3-D soil slope shown in Figure 3. Undrained shear strength, S_u, is considered to be lognormally distributed with mean of 30kPa and coefficient of variation (COV) of 0.3. The spatial variability of S_u is modeled using the squared exponential autocorrelation function with horizontal autocorrelation distance l_h = 20m and vertical autocorrelation distance l_v = 2m. Herein, the horizontal spatial variability is assumed to be isotropic in the lateral and axial directions. Besides, the unit weight of soil is taken as a deterministic value of 20kN/m^3.

Two FE models are developed for slope stability analysis, as shown in Figure 4. The FE mesh size measures 2m×2m×5m for the coarse FE model and 1m×1m×1m for the fine one. The elastic-perfectly plastic constitutive model with Mohr-Coulomb failure criterion is used in both

Table 1. Comparison of results between MCS-based RFEM and ARFEM.

Method		Total sample size, N_T		Failure sample size, N_F	Time (day)[a]		P_f	COV(P_f)	R (m^3)	Unit COV
MCS-based RFEM		10,000		32	89.9		3.20×10^{-3}	0.18	7.00	18
ARFEM	Preliminary	1850	162[b]	398[c]	0.3[c]	1.4[c]	8.64×10^{-4} [c]	0.31[c]	1.64[c]	3.9
	Target	125		55[c]	1.1[c]		2.80×10^{-3} [c]		6.71[c]	

Note: [a] Estimated by parallel computing; [b] Equivalent number of fine FE analysis; [c] Estimated on 20 independent runs.

analyses. The safety factor, *FS*, of slope stability is calculated using shear strength reduction technique. For simplicity, the slope failure consequence, *C*, is approximately taken as the sliding mass volume, *V*, which is identified by k-means clustering method based on the node displacements obtained from the FE analysis (Huang et al., 2013). For better understanding the slope failure mechanism, several shape characteristics of the slip surface are also taken into consideration, such as sliding mass length, *L*, sliding mass width, *W*, and sliding mass depth, *D*, as defined in Figure 3. All these values are referred to the maximum value along one particular direction. Figure 4 also provides the results of deterministic slope stability analysis based on the mean value of S_u. The *FS* values calculated by coarse and fine FE models are 1.651 and 1.593, respectively. The coarse FE model slightly overestimates *FS* and underestimates the scale of sliding mass in all directions, but it takes much less computational time than the fine one (i.e., 48s vs. 35min by series computing).

To estimate the P_f and R for the slope example, twenty ARFEM runs are performed with $m = 4$, $N = 500$, and $p_0 = 0.1$ in preliminary analysis using the coarse FE model and $N_s = 25$ in target analysis using the fine FE model. Each ARFEM run contains 1850 coarse FE analyses and 125 fine FE analyses in total. Besides, a direct MCS-based RFEM run with 10,000 fine FE analyses is also carried out for validation. Their results are summarized in Table 1. The P_f and R estimated in the preliminary analysis of ARFEM are 8.64×10^{-4} and 1.64m^3, respectively, which are almost three and four times smaller than those (i.e., 2.80×10^{-3} and 6.71m^3) evaluated in the target analysis of ARFEM. The target estimates agree well with those (i.e., 3.20×10^{-3} and 7.00m^3) obtained from direct MCS-based RFEM. This validates the ARFEM.

With regard to the computational efficiency, the unit COV is taken as a measure in this study, which is defined as COV(P_f)$\times\sqrt{N_T}$ and accounts for the effect of number of samples used in simulation on the variation of reliability estimate (Au, 2007). As shown in Table 1, ARFEM only requires about 1/21 (i.e., $(3.9/18)^2$) of the computational effort for MCS-based RFEM to achieve the same computational accuracy. Specifically, the direct MCS-based RFEM takes about 3 months by parallel computing on a desktop computer with 8 GB RAM and one Intel Core i7 CPU clocked at 3.4 GHz, while ARFEM only requires about 1.4 days on the same computer. The latter is much more acceptable in practice. ARFEM significantly improves the computational efficiency by incorporating the information obtained from preliminary analysis with coarse FE model into target analysis with fine FE model. This potentially facilitates the practical

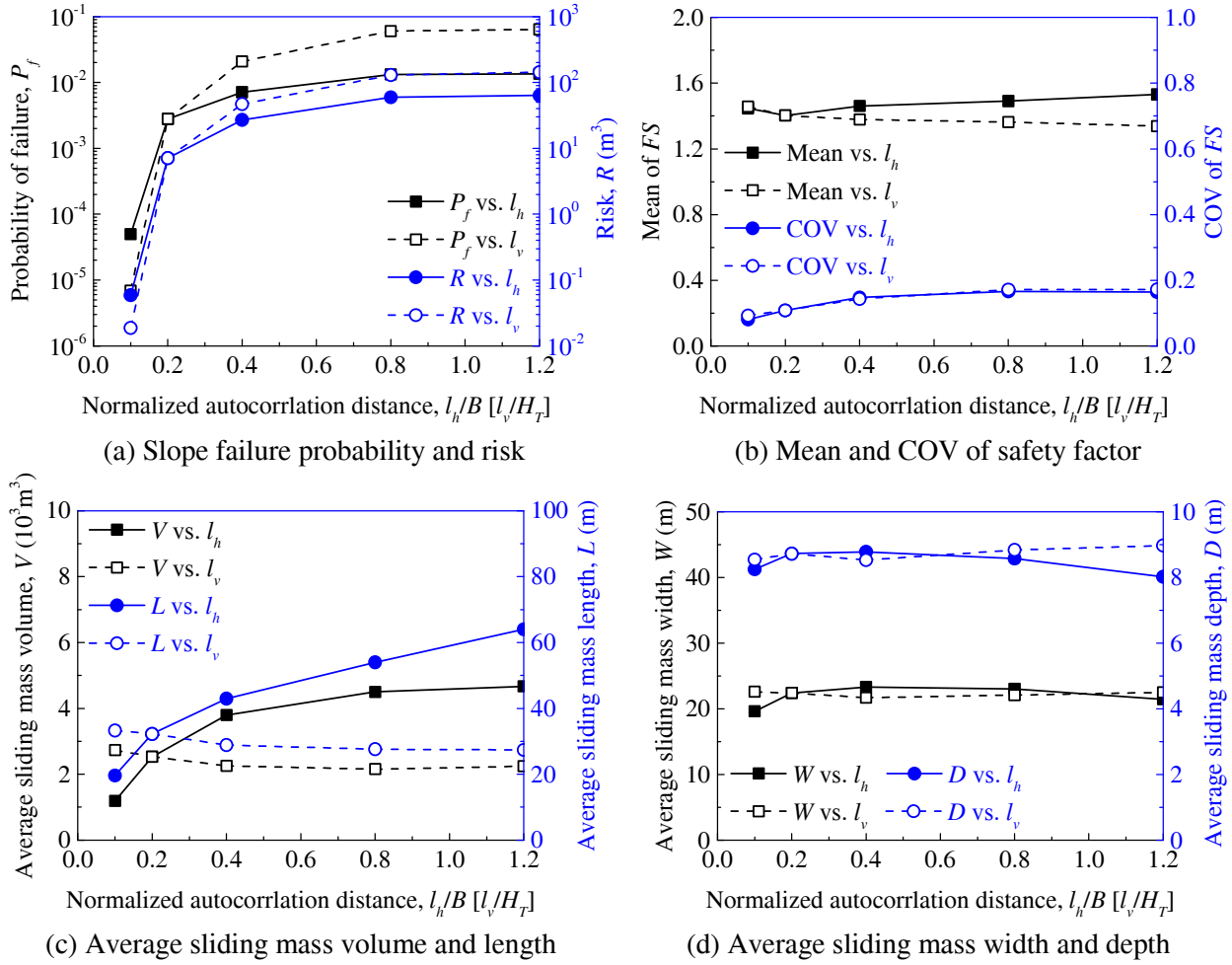

(a) Slope failure probability and risk

(b) Mean and COV of safety factor

(c) Average sliding mass volume and length

(d) Average sliding mass width and depth

Figure 5. Effects of spatial variability on 3-D slope.

application of RFEM in 3-D slope reliability analysis and risk assessment, particularly at small probability levels. In addition, ARFEM provides more failure samples (i.e., 55 failure samples among 125 representative samples) than direct MCS-based RFEM (i.e., 32 failure samples among 10,000 samples). This helps accurately estimate the slope failure consequence in risk assessment and better understand slope failure mechanisms, as discussed below.

EFFECTS OF SPATIAL VARIABILITY

With the aid of ARFEM, this section carries out a sensitivity study to systematically explore the effects of spatial variability on 3-D slope reliability, risk and failure mechanisms. In addition to the nominal case with l_h = 20m and l_v = 2m, eight cases with different autocorrelation distances are also considered, including four cases with l_h = [10, 40, 80, 120] m and l_v = 2m and four cases with l_h = 20m and l_v = [1, 4, 8, 12] m. For simplicity, all results presented in this section are obtained from the target analysis in ARFEM with fs = 1. To make a fair comparison, l_h and l_v are normalized by slope length B and nominal height H_T (see Figure 3), respectively.

Figure 5(a) shows the variation of slope failure probability and risk as a function of normalized autocorrelation distance. When normalized autocorrelation distance increases from 0.1 to 1.2, both P_f and R increase by serval orders of magnitude. The influence weakens when l_h exceeds half of the slope length or l_v exceeds the slope height. Besides, the vertical spatial variability has a greater impact on P_f and R than the horizontal spatial variability. By performing statistical analysis on FS (Xiao et al., 2016), it can be found that, for such a small probability problem, the increase in P_f is mainly attributed to the increase in variance of FS (see Figure 5(b)). This agrees with the conclusion drawn by Wang et al. (2011). As a matter of fact, the increasing variation of FS is further related to the spatial average phenomenon in spatially variable soils (Vanmarcke, 1977), which indicates that the variance for soil property along particular slip surface reduces as the autocorrelation distance decreases.

With respect to slope failure mechanisms, the variation of average volume, length, width and depth of sliding mass are shown in Figures 5(c) and 5(d). Apparently, the horizontal spatial variability and vertical spatial variability have opposite influences on average sliding mass volume and length in this example. Both of them increase as the normalized horizontal autocorrelation distance increases, and slightly decrease as the normalized vertical autocorrelation distance increases. The variation for average sliding mass volume is relatively smaller than that for P_f and R. Note that average sliding mass volume is equivalent to the average failure consequence $\bar{C}$ in this study. Therefore, R (i.e., $P_f \times \bar{C}$) is more sensitive to P_f than $\bar{C}$. Compared with the 2-D slope risk assessment (Li et al., 2016a), the effects of vertical spatial variability on P_f, $\bar{C}$ and R of 3-D slope are consistent with the observations in 2-D analysis. This implies the 2-D analysis can properly account for the vertical spatial variability.

In addition, since average sliding mass width and depth are almost unchanged as normalized autocorrelation distance varies in this example (see Figure 5(d)), the variation of sliding mass volume is dominated by the variation of sliding mass length. On the one hand, this indicates that the horizontal spatial variability in the axial direction, instead of that in the lateral direction, affects 3-D slope failure mechanism and average failure consequence. Since 2-D analysis can only account for the lateral spatial variability, rather than the axial one, the effect of horizontal spatial variability is commonly undervalued in previous literature based on 2-D analysis. Such an effect can be properly incorporated into 3-D slope risk assessment with 3-D spatial variability modeling. On the other hand, it also indicates that the horizontal spatial variability has a greater impact on slope failure mechanism than the vertical spatial variability. At least in this example, the vertical spatial variability has limited influence on all shape characteristics (i.e., volume, length, width and depth) of sliding mass. The location of sliding mass is dominated by the horizontal spatial variability as well.

During the sensitivity study, it is also interesting to note that the shape of slip surface differs as spatial variability varies, particularly the horizontal spatial variability. For 3-D slope stability analysis using limit equilibrium methods, an ellipsoidal slip surface (spherical in particular) or a cylindrical slip surface is widely assumed. They appear to be reasonable in some given conditions. Figure 6 demonstrates two random field realizations and corresponding slip

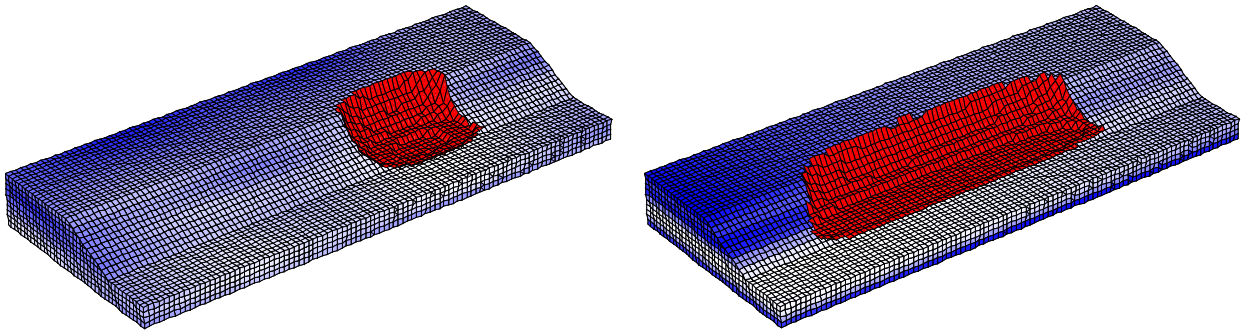

(a) Nearly-spherical (l_h = 20m, l_v = 2m) (b) Nearly-cylindrical (l_h = 80m, l_v = 2m)

Figure 6. Random field realizations and shapes of slip surface.

surfaces. The slip surface is nearly-spherical when the spatial variability is significant (i.e., small autocorrelation distance) (see Figure 6(a)), and it turns to be nearly-cylindrical when the spatial variability is weak (see Figure 6(b)). Therefore, it is difficult to determine the shape of slip surface in advance, especially when spatial variability of soil properties is considered. Improper assumption on the shape of slip surface may fail to locate the most dangerous failure mode and overestimate the safety factor of slope stability. Due to the 3-D FE analysis, there is no need to assume the shape and location of slip surface prior to the analysis in ARFEM.

CONCLUSIONS

This paper presented an auxiliary random finite element method (ARFEM) for efficient 3-D slope reliability analysis and risk assessment. A 3-D soil slope example was investigated to demonstrate the validity of ARFEM, and those results were verified by direct MCS-based RFEM. Results indicated that ARFEM significantly improves the computational efficiency by incorporating the information obtained from preliminary analysis with coarse FE model into target analysis with fine FE model. This potentially facilitates the practical application of RFEM in 3-D slope reliability analysis and risk assessment, particularly at small probability levels. In virtue of ARFEM, the effect of spatial variability on 3-D slope was explored. It was found that both the horizontal and vertical spatial variability have significant, but different, impacts on reliability, risk and failure mechanisms of 3-D slope. The slope reliability and risk are more dominated by the vertical spatial variability, while the slope failure mechanism, such as the volume, length and location of sliding mass, is more affected by the horizontal spatial variability.

ACKNOWLEDGMENTS

This work was supported by the National Natural Science Foundation of China (Project Nos. 51329901, 51409196, 51579190, 51528901), and the Natural Science Foundation of Hubei Province of China (Project No. 2014CFA001). The financial support is gratefully acknowledged.

REFERENCES

Au, S. K. (2007). "Augmenting approximate solutions for consistent reliability analysis." *Probabilist. Eng. Mech.*, 22(1), 77-87.

Au, S. K., and Wang, Y. (2014). *Engineering risk assessment with Subset Simulation*. Singapore: John Wiley & Sons.

Griffiths, D. V., and Fenton, G. A. (2004). "Probabilistic slope stability analysis by finite elements." *J. Geotech. Geoenviron.*, 130(5), 507-518.

Griffiths, D. V., Huang, J., and Fenton, G. A. (2009). "On the reliability of earth slopes in three dimensions." *Proc. Roy. Soc. Lond. A: Math., Phys. Eng. Sci.*, 465(2110), 3145-3164.

Hicks, M. A., Nuttall, J. D., and Chen, J. (2014). "Influence of heterogeneity on 3D slope reliability and failure consequence." *Comput. Geotech.*, 61, 198-208.

Huang, J., Lyamin, A. V., Griffiths, D. V., Krabbenhoft, K., and Sloan, S. W. (2013). "Quantitative risk assessment of landslide by limit analysis and random fields." *Comput. Geotech.*, 53, 60-67.

Jha, S. K., and Ching, J. (2013). "Simplified reliability method for spatially variable undrained engineered slopes." *Soils Found.*, 53(5), 708-719.

Ji, J., and Chan, C. L. (2014). "Long embankment failure accounting for longitudinal spatial variation–A probabilistic study." *Comput. Geotech.*, 61, 50-56.

Li, D. Q., Xiao, T., Cao, Z. J., Zhou, C. B., and Zhang, L. M. (2016a). "Enhancement of random finite element method in reliability analysis and risk assessment of soil slopes using Subset Simulation." *Landslides*, 13, 293-303.

Li, D. Q., Xiao, T., Cao, Z. J., Phoon, K. K., and Zhou, C. B. (2016b). "Efficient and consistent reliability analysis of soil slope stability using both limit equilibrium analysis and finite element analysis." *Appl. Math. Model.*, 40(9-10), 5216-5229.

Sudret, B., and Der Kiureghian, A. (2000). *Stochastic finite element methods and reliability: a state-of-the-art report*. Department of Civil and Environmental Engineering, University of California.

Vanmarcke, E. H. (1977). "Reliability of earth slopes." *J. Geotech. Eng. Divis.* 103(12), 1247-1265.

Wang, Y., Cao, Z., and Au, S. K. (2011). "Practical reliability analysis of slope stability by advanced Monte Carlo simulations in a spreadsheet." *Can. Geotech. J.*, 48(1), 162-172.

Xiao, T., Li, D. Q., Cao, Z. J., Au, S. K., and Phoon, K. K. (2016). "Three-dimensional slope reliability and risk assessment using auxiliary random finite element method." *Comput. Geotech.*, 79, 146-158.

Xiao, T., Li, D. Q., Cao, Z. J., and Tang, X. S. (2017). "Full probabilistic design of slopes in spatially variable soils using simplified reliability analysis method." *Georisk*, 11(1), 146-159.